# An X-ray Absorption Spectroscopic Study of Nickel Redox Chemistry in Hydrogenase

**Csaba Bagyinka,[†,‡] Joyce P. Whitehead,[†] and Michael J. Maroney*[,†,§]**

*Contribution from the Department of Chemistry and Program in Molecular and Cellular Biology, University of Massachusetts, Amherst, Massachusetts 01003*

*Received June 29, 1992*

**Abstract:** The results of X-ray absorption spectroscopic studies of *Thiocapsa roseopersicina* hydrogenase poised in three forms exhibiting EPR signals due to the Ni center (A, B, and C) and two states that are epr silent with respect to the Ni center are reported. These spectra are used to examine the structural changes that occur during the reduction of the enzyme. Analyses of Ni K-edge spectra reveal the presence of weak features at ca. 8332 eV in the spectra obtained from forms A and B and the silent intermediate (SI) that are assigned to 1s → 3d transitions. The lack of a significant pre-edge peak in the active form of the enzyme and low peak areas in other forms, coupled with the absence of edge features associated with planar four-coordinate Ni complexes, indicate that the Ni site in all states of the enzyme is five- or six-coordinate. No observable shift in edge energy occurs upon reduction of the enzyme to any level. This demonstrates that no significant change in the electron density of the Ni site occurs during reduction. Analyses of the EXAFS spectra obtained from scattering atoms in the first coordination sphere of Ni in all five states of the enzyme that are defined by Ni EPR signals (or lack thereof) are consistent with a Ni site composed of 3 ± 1 N(O)-donors at 2.00 ± 0.06 Å and 2 ± 1 S-donors at 2.23 ± 0.03 Å. These results are discussed in light of various models for the structure and function of the Ni site in the enzyme. No evidence to support a redox role for Ni in hydrogenase is found in the XAS data.

Hydrogenases ($H_2$ases) are a diverse group of enzymes found in both prokaryotes and eukaryotes that catalyze the reversible two-electron oxidation of molecular hydrogen.[1-3] Thus, $H_2$ases may function to provide reducing equivalents for energy production via the uptake and oxidation of $H_2$ or they may reduce $H^+$ in the production of $H_2$. Hydrogen oxidation (uptake) is generally coupled with phosphorylation and ultimately to the reduction of inorganic substrates such as $SO_4^{2-}$ (*Desulfovibrio* species),[4] $CO_2$ (*Methanobacterium* species),[5] $NO_3^-$ (e.g. *Paracoccus denitrificans*),[6,7] or $O_2$ (*Alcaligenes* and *Nocardia*).[6,8,9] $H_2$ases may also play a role in cycling hydrogen produced in other systems (e.g. nitrogenase) or in generating a proton gradient.[10]

Hydrogenases have been grouped into three classes, based on the inorganic content of the enzymes, that are immunologically and biochemically distinct.[11-13] With the apparent exception of a recently purified enzyme, $N^5$,$N^{10}$-methylenetetrahydromethanopterin dehydrogenase from *Methanobacterium thermoautotrophicum* that possesses $H_2$ase activity but does not contain Fe,[14] all $H_2$ases contain Fe,S clusters. One class, the Fe-only enzymes, contains only Fe and sulfide.[1] Since the discovery of Ni as a biological component of *Methanobacterium bryantii* in 1980[15] and the subsequent identification of the Ni-containing component as a $H_2$ase,[16] many examples of $H_2$ases that require a single Ni atom as well as Fe,S clusters have been characterized. $H_2$ases belonging to the Fe,Ni class are generally associated with hydrogen oxidation in vivo and are by far the most common and widely distributed form of the enzyme; examples are known from fermentative,[17] $SO_4$-reducing,[4,18] methanogenic,[5] photosynthetic,[10,19] facultative,[20] and aerobic bacteria.[21,22] Among the $H_2$ases containing Ni are a class of enzymes that contain Se as well—the Fe,Ni,Se $H_2$ases.[18] The Se is generally present as a single selenocysteine residue, most notably in *D. baculatus*, where it has been shown to be encoded by an internal TGA codon,[23] and constitutes a conservative replacement for a cysteine residue in enzymes lacking selenocysteine.[23] Spectroscopic studies have shown this selenocysteine to be one of the Ni ligands.[24,25]

When Ni is present in the enzyme, it is often detected by an unusual rhombic $S = {}^1/_2$ EPR signal ($g = 2.4$–$2.0$) that has been

† Department of Chemistry.
‡ Current Address: Biological Research Center of the Hungarian Academy of Sciences, H-6701, Szeged, Hungary.
§ Program in Molecular and Cellular Biology.

(1) Adams, M. W. W. *Biochim. Biophys. Acta* **1990**, *1020*, 115–45.
(2) Cammack, R.; Hall, D. O.; Rao, K. K. In *Microbial Gas Metabolism: Mechanistic, Metabolic and Biotechnical Aspects*; Poole, K. K., Dow, C. Eds.; Academic Press: London, 1985; Chapter 4.
(3) Przybyla, A. E.; Robbins, J.; Menon, N.; Peck, H. D. *FEMS Microbiol. Rev.* **1992**, *88*, 109–35.
(4) Hatchikian, E. C.; Fernandez, V. M.; Cammack, R. *FEMS Symp.* **1990**, *54*, 53–73.
(5) Bastian, N. R.; Wink, D. A.; Wackett, L. P.; Livingston, D. J.; Jordan, L. M.; Fox, J.; Orme-Johnson, W. H.; Walsh, C. T. In *The Bioinorganic Chemistry of Nickel*; Lancaster, J. R., Jr., Ed.; VCH: New York, 1988; pp 227–47.
(6) Knuttel, K.; Schneider, K.; Schlegel, H. G.; Muller, A. *Eur. J. Biochem.* **1989**, *179*, 101–8.
(7) Sim, E.; Vignais, P. M.; *Biochimie* **1978**, *60*, 307–14.
(8) Schink, B.; Schlegel, H. G. *Biochemie* **1978**, *60*, 297–305.
(9) Doyle, C. M.; Arp, D. J. *J. Bacteriol.* **1987**, *169*, 4463–8.
(10) Vignais, P. M.; Colbeau, A.; Willison, J. C.; Jouanneau, Y. *Adv. Microb. Physiol.* **1985**, *26*, 155–234.
(11) Kovacs, K. L.; Seefeldt, L. C.; Tigyi, G.; Doyle, C. M.; Mortensen, L. E.; Arp, D. J. *J. Bacteriol.* **1989**, *171*, 430–5.
(12) Fauque, G.; Teixeira, M.; Moura, I.; Lespinat, P. A.; Xavier, A. V.; Der, V. D.; Peck, H. J.; Le, G. J.; Moura, J. G. *Eur. J. Biochem.* **1984**, *142*, 21–8.
(13) Lorenz, B.; Schneider, K.; Kratzin, H.; Schlegel, H. G. *Biochim. Biophys. Acta* **1989**, *995*, 1–9.
(14) Zirngibl, C.; Hedderich, R.; Thauer, R. K. *FEBS Lett.* **1990**, *261*, 112–16.
(15) Lancaster, J. R., Jr. *FEBS Lett.* **1980**, *115*, 285–88.
(16) Albracht, S. P.; Graf, E. G.; Thauer, R. K. *FEBS Lett.* **1982**, *140*, 311–3.
(17) Bryant, F. O.; Adams, M. W. *J. Biol. Chem.* **1989**, *264*, 5070–9.
(18) Fauque, G.; Peck, H. D., Jr.; Moura, J. J. G.; Huynh, B. H.; Berlier, Y.; DerVartanian, D. V.; Teixeira, M.; Przybyla, A. E.; Lespinat, P. A.; Moura, I.; LeGall, J. *FEMS Microbiol. Rev.* **1988**, *54*, 299–344.
(19) Gogotov, I. N. *Biochemie* **1986**, *68*, 181–7.
(20) Ballantine, S. P; Boxer, D. H. *J. Bacteriol.* **1985**, *163*, 454–9.
(21) Cammack, R.; Fernandez, V. M.; Schneider, K. In *The Bioinorganic Chemistry of Nickel*; Lancaster, J. R., Jr., Ed.; VCH: New York, 1988; Chapter 8.
(22) Seefeldt, L. C.; Arp, D. J. *Biochimie* **1986**, *68*, 25–34.
(23) Voordouw, G.; Menon, N. K.; LeGall, J.; Choi, E. S.; Peck, H. J.; Przybyla, A. E. *J. Bacteriol.* **1989**, *171*, 2894–9.
(24) Eidsness, M. K.; Scott, R. A.; Prickril, B. C.; DerVartanian, D. V.; Legall, J.; Moura, I.; Moura, J. J.; Peck, H. J. *Proc. Natl. Acad. Sci. U.S.A.* **1989**, *86*, 147–51.

0002-7863/93/1515-3576$04.00/0 

**Table I.** Amino Acid Analysis of *Thiocapsa roseopersicina* Hydrogenase

| amino acid | $X \pm \sigma^a$ | Kovacs et al.[31] | amino acid | $X \pm \sigma^a$ | Kovacs et al.[31] |
|---|---|---|---|---|---|
| Asp | 103.0 ± 3.1 | 136 | Tyr | 30.5 ± 1.7 | 4 |
| Glu | 80.5 ± 5.4 | 48 | Val | 66.5 ± 1.5 | 60 |
| Ser | 43.2 ± 2.8 | 68 | Met | 21.3 ± 0.9 | 4 |
| Gly | 84.0 ± 3.3 | 136 | Ile | 49.5 ± 1.8 | 32 |
| His | 18.5 ± 2.1 | 20 | Leu | 87.8 ± 2.9 | 54 |
| Arg | 57.2 ± 1.5 | 25 | Phe | 32.7 ± 1.8 | 18 |
| Thr | 50.8 ± 0.4 | 44 | Lys | 32.0 ± 4.1 | 19 |
| Ala | 105.2 ± 1.5 | 124 | Cys | 12.5 ± 0.5 | 4 |
| Pro | 48.2 ± 4.8 | 50 | Trp | | |

[a] Based on the analysis of four samples except for cysteine/cystine, which is based on two samples. Analysis was not performed for Trp.

assigned to formally Ni(III) or Ni(I) centers.[26,27] Distinct EPR signals are observed for the oxidized and catalytically inactive forms of the enzyme (forms A and B), as well as in a reduced and active form (form C). These EPR signals have provided a principal spectroscopic probe of the Ni site and have been used to demonstrate the redox activity of the site.[21,26,28] Under $H_2$ atmosphere, the signals associated with the oxidized forms disappear, yielding a redox state of the enzyme that is EPR silent at 77 K (silent intermediate, SI). Further exposure to $H_2$ causes the signal associated with the active form of the enzyme to appear. Extensive incubation of the enzyme under $H_2$ leads to the formation of the fully reduced form (R) of the enzyme, which is also EPR silent. Various schemes employing formal Ni oxidation states IV–0 have been used to account for the appearance and disappearance of EPR signals associated with the Ni site.[5,21,26,28,29] Using samples of *Thiocapsa roseopersicina* $H_2$-ase, a typical Fe,Ni enzyme,[19,21,30–32] poised with respect to the Ni EPR signals, we report here the results of a Ni K-edge X-ray absorption spectroscopic study of the structure of the Ni site in each form of the enzyme. This study reveals structures for the Ni site that are remarkably *insensitive* to the redox state of the enzyme and are therefore inconsistent with Ni-centered redox chemistry.

## Results

**Enzymology.** Samples of *Thiocapsa roseopersicina* $H_2$ase were analyzed for amino acid content in order to obtain an accurate measure of the protein concentration of samples used in the XAS study. The results of these analyses are summarized in Table I. Two previous analyses of the amino acid content of this enzyme have appeared in the literature[30,32] and are not in agreement with each other regarding the amino acid content of the enzyme. Our results do not agree with either of the previously published determinations. Nonetheless, the analyses reported here are reproducible and provide an estimate of the molecular weight of the protein of 98.0 kDa, which is in agreement with published values.[32] The electronic absorption spectra of the samples that were analyzed for amino acid content were used to obtain extinction coefficients for the enzyme at 220 nm (895 000 $cm^{-1}$ $M^{-1}$) and 280 nm (106 000 $cm^{-1}$ $M^{-1}$). Using the absorbance at 220 nm and BSA as a standard to calculate the protein concentration of the samples leads to values that are 84.7% of the total protein amount determined by the amino acid analysis. A correction factor of 1.18 was therefore applied to the apparent concentration of $H_2$ase determined using spectrophotometric measurements and a standard BSA calibration curve.[33]

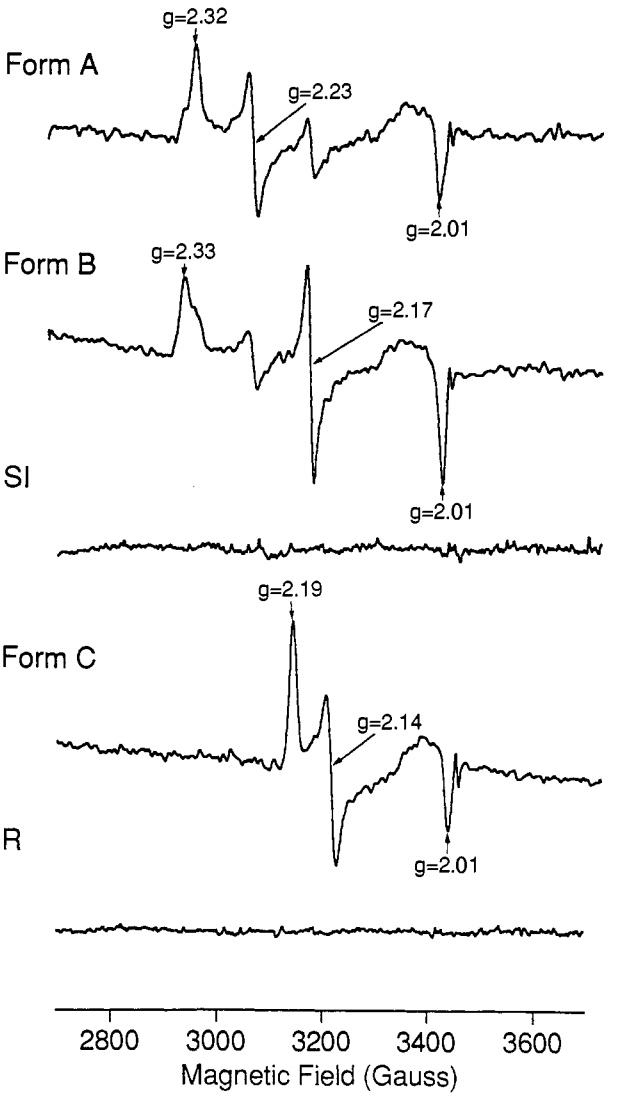


**Figure 1.** Nickel EPR spectra of *Thiocapsa roseopersicina* hydrogenase XAS samples prior to exposure to synchrotron radiation. The spectra were recorded at 77 K, with microwave power of 20 mW, at a frequency of 9.62 GHz, and a modulation amplitude of 4 G.

Metal analyses were performed on a portion of the samples analyzed for amino acid content and on samples where the concentration of the protein was determined spectrophotometrically. These analyses reveal that the enzyme contains 1.0 ± 0.1 Ni atoms and 8.0 ± 1.0 Fe atoms per molecule, in agreement with previously determined Ni:Fe ratios.[31,33]

Samples of *T. roseopersicina* $H_2$ase were poised with respect to the Ni EPR signal at 77K using the procedures described in the Experimental section. These samples were frozen in polycarbonate holders and the EPR spectra of the samples before exposure to synchrotron radiation were measured. Representative spectra are shown in Figure 1. Redox levels that have Ni EPR signals, where we can ascertain that the majority of the

(25) He, S. H.; Teixeira, M.; LeGall, J.; Patil, D. S.; Moura, I.; Moura, J. J.; DerVartanian, D. V.; Huynh, B. H.; Peck, H. J. *J. Biol. Chem.* **1989**, *264*, 2678–82.
(26) Moura, J. J. G.; Teixeira, M.; Moura, I.; LeGall, J. In *The Bioinorganic Chemistry of Nickel*; Lancaster, J. R., Jr., Ed.; VCH: New York, 1988; pp 191–226.
(27) Moura, J. J. G.; Teixeira, M.; Xavier, A. V.; Moura, I.; LeGall, J. *J. Mol. Catal.* **1984**, *23*, 303.
(28) van der Zwaan, J. W.; Albracht, S. P.; Fontijn, R. D.; Slater, E. C. *FEBS Lett.* **1985**, *179*, 271–7.
(29) Coremans, J. M. C. C.; VanderZwaan, J. W.; Albracht, S. P. *J. Biochim. Biophys. Acta* **1989**, *997*, 256–67.
(30) Gogotov, I. N.; Zorin, N. A.; Serebriakova, L. T.; Kondratieva, E. N. *Biochim. Biophys. Acta* **1978**, *523*, 335–43.
(31) Kovacs, K. L.; Bagyinka, C. *FEMS Microbiol. Rev.* **1990**, *87*, 407–11.
(32) Kovacs, K. L.; Tigyi, G.; Thanh, L. T.; Lakatos, S.; Kiss, Z.; Bagyinka, C. *J. Biol. Chem.* **1991**, *266*, 947–51.
(33) Maroney, M. J.; Colpas, G. J.; Bagyinka, C.; Baidya, N.; Mascharak, P. K. *J. Am. Chem. Soc.* **1991**, *113*, 3962–72. (The estimate of the redox poise of the form C sample used in this previous study has been corrected from 95% to 80% based on the better determination of the protein content of the sample available from amino acid analysis.)

**Table II.** EPR and Ni K-Edge Data

| enzyme redox state | Ni K-edge energy ±0.2 (eV) | 1s → 3d peak area ± 0.005 eV (rel to $NiCl_4^{2-}$)[38] | S/N | % Ni EPR detectable | % of EPR active Ni poised |
|---|---|---|---|---|---|
| form A(1) | 8339.6 | 0.006 (0.05) | 106.34 | 85 | 80 |
| form A(2) | 8340.4 | 0.015 (0.132) | 549.48 | 91 | 78 |
| form A(3) | 8340.5 | 0.010 (0.088) | 12.16 | 91 | 95 |
| form B(1) | 8339.4 | 0.040 (0.351) | 409.93 | 90 | 85 |
| form B(2) | 8339.8 | 0.015 (0.132) | 308.38 | 96 | 80 |
| SI | 8339.8 | 0.014 (0.123) | 465.24 | 0 | (100) |
| form C(1) | 8339.3 | <0.001 (0) | 20.56 | 80 | 100 |
| form C(2) | 8339.6 | <0.001 (0) | 666.15 | 80 | 100 |
| R | 8339.5 | 0.007 (0.061) | 1018.21 | 0 | (100) |

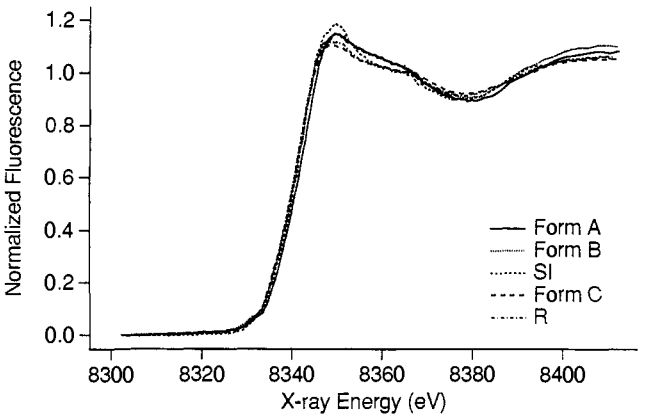


**Figure 2.** Ni K-edge XANES spectra of all five redox states of the $H_2$ase from *T. roseopersicina*.

Ni in the sample is in a single complex, are designated as "forms". Integration of the EPR signals indicates that 80–100% of the Ni in the samples poised in forms A, B, and C is present in an EPR active form (Table II). For samples poised in the oxidized forms A and B, the EPR spectra account for 100% of the Ni content and reveal the presence of a small amount of the unintended oxidized form. Simulations of the EPR spectra using parameters from poised samples indicate that the minor component in the XAS samples accounts for less than ca. 20% of the EPR active Ni in any sample. Form C samples containing 80% of the Ni in the enzyme poised in form C were prepared. Since form C is bracketed by EPR silent states, the oxidation state of ca. 20% of the sample is undetermined. No change in the Ni EPR signals from any sample was noted following exposure to synchrotron radiation. Samples containing EPR silent Ni species were EPR silent with respect to the Ni center before and after exposure, but these are not designated as "forms" because of the lack of a probe of the Ni site that would reveal a possible mixture of EPR silent Ni species.

**Ni K-Edge Studies.** The edge regions of Ni K-edge XAS spectra obtained on redox-poised samples of *T. roseopersicina* $H_2$ase are shown in Figure 2. These spectra are quite similar and do not reveal any significant changes in energy or structure as a function of the oxidation level of the enzyme. Values for the edge energy and pre-edge peak areas obtained from several $H_2$ase samples are contained in Table II. The pre-edge region of the spectra shows no evidence of a peak or shoulder near 8338 eV that has been assigned to a 1s → $4p_z$ transition (with shakedown contributions)[34-37] that is observed in the XAS spectra of planar four-coordinate complexes and pyramidal five-coordinate complexes.[38,39] In several cases, it is possible to resolve a weak peak near 8332 eV that has been assigned to a 1s → 3d transition.[39-41] The 1s → 3d transition is symmetry-forbidden in centrosymmetric point groups, but it is expected to gain intensity in geometries that allow p–d mixing to occur.[38,42] With the exception of one form B sample, which appears to be anomalous, all of the areas observed for the 1s → 3d peaks range from 0 to 0.015(5) eV, or ratios of 0–0.13 relative to the area of the $(Et_4N)_2[NiCl_4]$ pre-edge peak.[38] The low intensity of this feature in the $H_2$ase spectra is consistent with either a planar four-coordinate geometry (peak areas of 0–0.029(5) eV[38]) or a six-coordinate geometry (peak areas of 0.006(5)–0.040(5) eV[38]). For the single form B sample that lies outside this range (0.040(5) eV), a five-coordinate Ni site (peak areas of 0.042(5)–0.096(5) eV[38]) is also consistent with the data. Given the absence of a 1s → $4p_z$ transition that is expected for the planar and pyramidal geometries, the spectra obtained from all of the $H_2$ase samples are most consistent with a six-coordinate Ni, although a five-coordinate trigonal-bipyramidal site is also a possibility.

The post-edge XANES region is remarkably constant and indicates that there are no changes in the Ni–ligand environment or the Ni–ligand bond lengths as a function of redox state.

**Ni EXAFS Spectra.** Fourier-filtered first-coordination-sphere (backtransform window = 1.1–2.7 Å) EXAFS data were fit to obtain information regarding changes in ligation of the Ni or Ni–ligand bond lengths that might occur as a function of redox state of the enzyme. The restricted fit protocol, which constrains coordination number to integer values and adjusts only the metal–ligand bond distance ($r$) and a disorder parameter ($\sigma$), was employed to generate all possible fits involving one or two shells of scattering atoms. A complete table of these results is available as supplementary material. The best fits, as judged by minimizing both the value of $R$ and $|\Delta\sigma^2|$ (see Experimental Section), are shown in Table III and Figures 3–5. These fits reveal that no significant change in either the ligand environment of the $H_2$ase Ni center or the average Ni–ligand bond lengths occurs as a function of the redox state of the enzyme. In general, the EXAFS spectra are not fit well using only a single shell of either N(O) or S(Cl) scattering atoms. All of the EXAFS spectra may be fit using a combination of 3 ± 1 N(O) atoms at 2.00 ± 0.06 Å and 2 ± 1 S(Cl) atoms at 2.23 ± 0.03 Å.

Although the number of scattering atoms is poorly determined by EXAFS analysis,[33] the best fits obtained from a two-shell analysis generally indicate a Ni coordination number of five, in contrast to the edge analysis which is most consistent with six-

(34) Smith, T. A.; Penner-Hahn, J. E.; Berding, M.; Doniach, S.; Hodgson, K. O. *J. Am. Chem. Soc.* **1985**, *107*, 5945–55.
(35) Bair, R. A.; Goddard, W. A. *Phys. Rev. B* **1980**, *2767–76*.
(36) Kosugi, N.; Yokohama, T.; Asakura, K.; Kuroda, H. *Chem. Phys.* **1984**, *91*, 249–56.
(37) Yokoyama, T.; Kosugi, N.; Kuroda, H. *Chem. Phys.* **1986**, *103*, 101–9.
(38) Colpas, G. J.; Maroney, M. J.; Bagyinka, C.; Kumar, M.; Willis, W. S.; Suib, S. L.; Mascharak, P. K.; Baidya, N. *Inorg. Chem.* **1991**, *30*, 920–8.
(39) Eidsness, M. K.; Sullivan, R. J.; Scott, R. A. In *The Bioinorganic Chemistry of Nickel*; Lancaster, J. R., Jr., Ed.; VCH: New York, 1988; pp 73–91.
(40) Schulman, R. G.; Yafet, Y.; Eisenburger, P.; Blumberg, W. E. *Proc. Natl. Acad. Sci. U.S.A.* **1976**, *73*, 1384–88.
(41) Hahn, J. E.; Scott, R. A.; Hodgson, K. O.; Doniach, S.; Desjardins, S. E.; Soloman, E. I. *Chem. Phys. Lett.* **1982**, *88*, 595–98.
(42) Roe, A. L.; Schneider, D. J.; Mayer, R. J.; Pyrz, J. W.; Widom, J.; Que, L., Jr. *J. Am. Chem. Soc.* **1984**, *106*, 1676–81.

**Table III.** Analysis of First Coordination Sphere Fourier-Filtered EXAFS Spectra

| redox state | no. of shells | $N^a$ | $r$ (Å)$^b$ | $\Delta\sigma^2$ ($\times 10^3$ Å$^2$)$^c$ | correl >0.6 | $R^d$ |
|---|---|---|---|---|---|---|
| form A(1) | 1 | 5 | Ni–N = 2.031(3) | 0.7 | | 0.731 |
| | | 5 | Ni–S = 2.223(4) | 11.4 | | 0.840 |
| | 2 | 4 | Ni–N = 2.015(5) | 5.9 | | 0.458 |
| | | 1 | Ni–S = 2.208(4) | –0.2 | | |
| form A(2) | 1 | 5 | Ni–S = 2.207(2) | 10.2 | | 0.531 |
| | 2 | **3** | **Ni–N = 1.972(3)** | **0.5** | $r_N/\sigma_S$ = **0.64** | **0.368** |
| | | **2** | **Ni–S = 2.227(3)** | **3.9** | | |
| | | 2 | Ni–N = 1.971(4) | –0.6 | $r_N/\sigma_S$ = 0.62 | 0.300 |
| | | 3 | Ni–S = 2.221(2) | 6.8 | | |
| form B(1) | 1 | 5 | Ni–N = 2.071(5) | –3.3 | | 1.866 |
| | 2 | 4 | Ni–N = 1.977(2) | 1.2 | | 0.332 |
| | | 1 | Ni–S = 2.238(7) | –7.3 | | |
| form B(2) | 1 | 5 | Ni–S = 2.221(2) | 9.2 | | 0.495 |
| | 2 | **3** | **Ni–N = 1.954(2)** | **2.2** | | **0.186** |
| | | **2** | **Ni–S = 2.239(8)** | **0.6** | | |
| SI | 1 | 4 | Ni–S = 2.242(2) | 9.5 | | 0.543 |
| | 2 | **2** | **Ni–N = 2.034(8)** | **2.7** | $r_N/\sigma_S$ = **–0.70** | **0.363** |
| | | **3** | **Ni–S = 2.244(3)** | **6.3** | | |
| | | 3 | Ni–N = 2.019(5) | 2.2 | $r_S/\sigma_N$ = –0.66 | 0.435 |
| | | 2 | Ni–S = 2.254(3) | 3.2 | | |
| form C(1) | 1 | 5 | Ni–N = 2.058(2) | –5.9 | | 1.079 |
| | 2 | 3 | Ni–N = 2.060(3) | –5.6 | $r_N/r_S$ = –0.82 | 0.481 |
| | | 2 | Ni–S = 2.209(3) | 0.6 | $\sigma_N/\sigma_S$ = –0.80 | |
| Form C(2) | 1 | 4 | Ni–S = 2.231(2) | 6.7 | | 0.603 |
| | 2 | 2 | Ni–N = 2.065(2) | 5.6 | $r_N/r_S$ = –0.78 | 0.587 |
| | | 3 | Ni–S = 2.225(4) | 5.6 | $\sigma_N/\sigma_S$ = –0.83 | |
| | | **2** | **Ni–N = 2.012(6)** | **–2.8** | $r_N/\sigma_S$ = **0.64** | **0.604** |
| | | **2** | **Ni–S = 2.250(4)** | **2.0** | $r_S/\sigma_N$ = **–0.66** | |
| R | 1 | 4 | Ni–S = 2.236(2) | 6.4 | | 0.582 |
| | 2 | **2** | **Ni–N = 2.029(7)** | **0.9** | $r_N/\sigma_S$ = **0.67** | **0.498** |
| | | **2** | **Ni–S = 2.243(4)** | **2.1** | $r_S/\sigma_N$ = **–0.67** | |
| | | 2 | Ni–N = 2.076(9) | 1.0 | $r_N/r_S$ = –0.80 | 0.436 |
| | | 3 | Ni–S = 2.227(3) | 5.9 | $\sigma_S/\sigma_N$ = –0.85 | |

$^a$ $N$ is the number of identical scattering atoms (restricted to integer values). $^b$ $r$ is the bond lengths. $^c$ $\Delta\sigma^2 = (\sigma^2_{fit} - \sigma^2_{model})$. $^d$ $R = [\sum k^6(\chi_c - \chi)^2/n]^{1/2}$.

coordinate Ni sites. Therefore, the possibility of a third shell of scattering atoms was addressed. The two shell fits obtained from Fourier-filtered data for form A and SI and R are improved by the addition of an S scattering atom at a longer distance (2.4–2.7 Å, supplementary material). The data will not accommodate an Fe atom at this distance. The data for forms B and C can accommodate a long S scatterer, but the fits are not significantly improved by the addition of the third shell.

To avoid problems associated with truncation errors in fits generated using Fourier-filtered data, the unfiltered EXAFS data were also fit using the same procedure. The best fits are summarized in Figure 5 and Table IV. A complete set of fits generated using unfiltered data is available as supplementary material. For the N(O) and S scattering atoms in the first two shells, the fits are in excellent agreement with those obtained using Fourier-filtered data. Although the bond lengths refined for the third shell S scatterer in the fits of unfiltered data are in agreement with those found using Fourier-filtered data, there is no significant improvement in the value of $R$ upon the addition of the third shell S atom. Thus, although the data are consistent with the presence of a long S-scattering atom, there is no compelling evidence for its existence from EXAFS analysis.

The effects on the EXAFS fits due to the presence of two forms of Ni in the oxidized forms of the enzyme were also explored. Using the results from spectral subtraction of the EPR spectra obtained for samples poised in forms A and B, the spectra of the oxidized forms were corrected for the presence of the impurity by subtracting the XAS spectrum of the oxidized sample in question. The resulting spectrum was normalized and the EXAFS data were analyzed. No significant effect due to the presence of a small amount of the other oxidized form was apparent from a composition of these fits. A complete set of fits to corrected data is available as supplementary material.

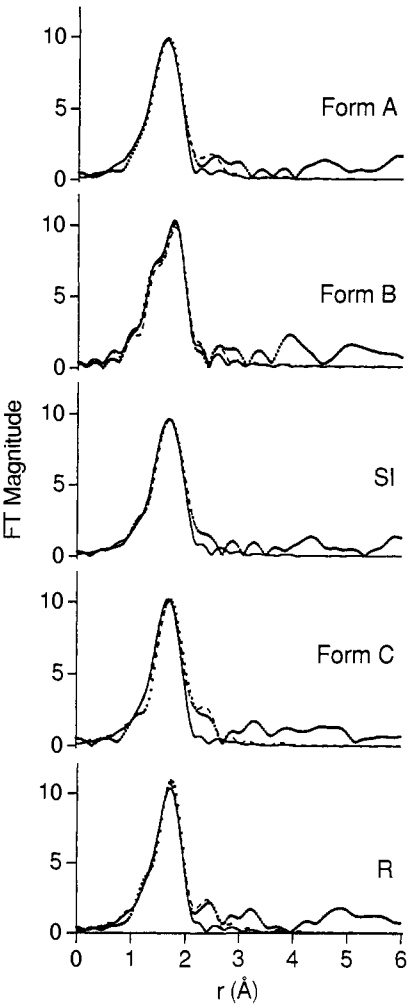


**Figure 3.** Fourier-transformed Ni K-edge EXAFS spectra from *T. roseopersicina* $H_2$ase (—) and the 2-shell (···) and 3-shell (– –) fits generated by using Fourier-filtered data with a backtransform window of 1.1–2.7 Å. The 2-shell fits shown are from Table III (boldface type). Note the small additional feature that is fit by the inclusion of a long S-donor atom in the 3-shell fits.

## Discussion

The presence of Ni in most hydrogenases is revealed by an unusual EPR signal arising from an $S = {}^1/_2$ center. Since Ni(II) contains an even number of electrons, the observation of an $S = {}^1/_2$ EPR signal in Fe,Ni $H_2$ases that reveals hyperfine arising from $^{61}$Ni in isotopically labeled samples led to proposals that unusual oxidation states of Ni (III or I) were stabilized in this enzyme.[21,26,28] When Fe,Ni $H_2$ases are isolated in air, oxidized and catalytically inactive samples are obtained. These samples exhibit two distinct EPR signals arising from Ni centers in the enzyme (signals A and B) and are therefore a mixture of two distinct forms of $H_2$ase (e.g. Figure 1). The proportion of forms A and B in an oxidized sample is dependent upon the oxidation process, and it is possible to manipulate the enzyme such that all or most of the sample exhibits a single EPR signal.[43] The similarity of the EPR signals obtained from $H_2$ases from a variety of sources,

(43) van der Zwaan, J. W.; Coremans, J. M. C. C.; Bouwens, E. C. M.; Albracht, S. P. J. *Biochim. Biophys. Acta* **1990**, *1041*, 101–10.

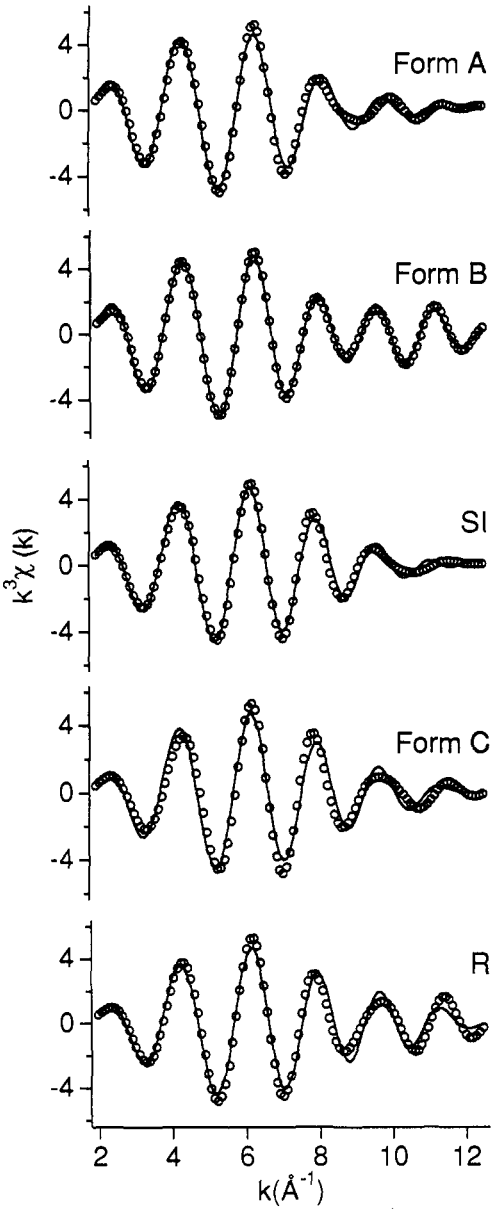


Figure 4. First coordination sphere (backtransform window = 1.1–2.7 Å) Fourier-filtered Ni K-edge EXAFS spectra of *T. roseopersicina* $H_2$ase samples (o) and 2-shell (–) fits from Table III (boldface type).

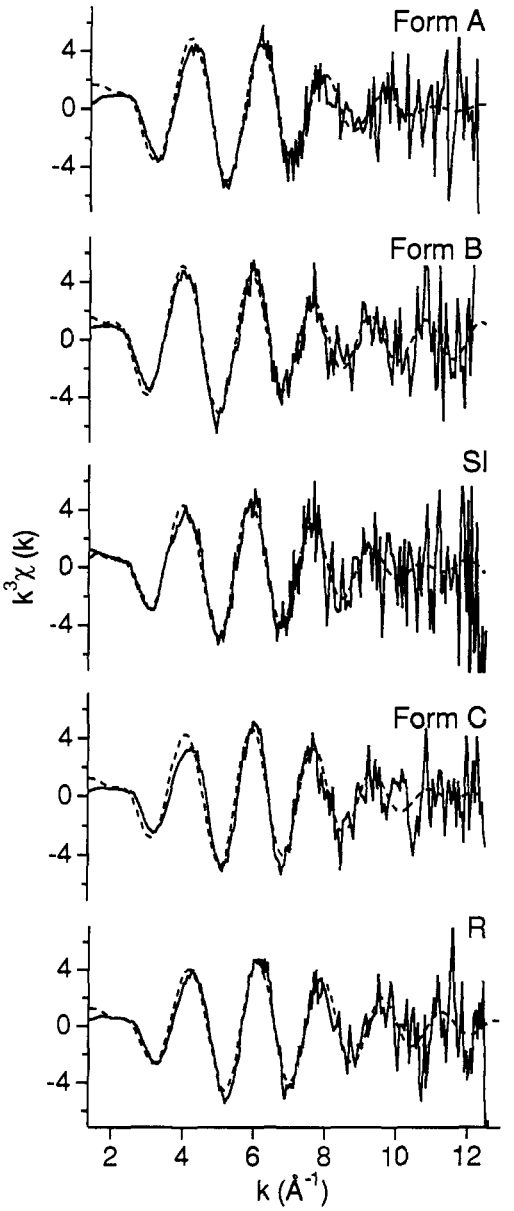


Figure 5. The $k^3$-weighted unfiltered EXAFS data (—) and 2-shell (···) fits. The fits are from Table IV (boldface type).

including both chemotrophic and phototrophic bacteria, suggests that similar Ni sites exist in all of these enzymes.[21,44] Nonetheless, differences in the chemistry associated with the Ni sites exist. In the case of *Thiocapsa roseopersicina* $H_2$ase, the enzyme as isolated in air exists mostly in form B. In this regard, *T. roseopersicina* $H_2$ase differs from the other $H_2$ases (e.g. *Desulfovibrio gigas*,[45] *Azotobacter vinlandii*,[46] *Methanobacterium thermoautotrophicum*[29,47]), where form A is the major form of the enzyme as isolated in air. It is similar to other $H_2$ases that are isolated in primarily form B (e.g. *Desulfovibrio fructosovorans*,[48] *Desulfovibrio desulfuricans*,[45] *Spirillum* 5175[49]). However, form B is converted to form A upon standing—even at 77 K, although the process takes several weeks at low temperature.

Incubation of oxidized and catalytically inactive enzymes under $N_2$ or Ar atmospheres containing $H_2$ leads to the disappearance of the EPR signals associated with oxidized enzymes. Following the formation of an EPR silent intermediate (SI), a new Ni EPR signal (signal C) appears that is associated with a catalytically active form (form C) of the enzyme.[21,26] Extensive incubation of the enzyme under $H_2$ leads to a reduced form (R) that has no Ni EPR signal and is not catalytically active. Redox titrations reveal that the redox chemistry associated with the five forms of the enzyme defined by Ni EPR spectroscopy occurs at potentials between ca. 0 and –400 mV. (For example, potentials obtained from redox titrations of *Desulfovibrio gigas* $H_2$ase are shown in Table V.)

The sequential appearance and disappearance of EPR signals associated with the Ni site upon exposure to $H_2$, or with increasingly, negative potentials, suggests that Ni redox chemistry might be involved. Schemes involving Ni formal oxidation states of IV to 0 have been proposed to account for the behavior of the Ni EPR signals.[5,21,26,29,43] Two of these proposals are summarized in Table V. Proposal A assigns a formal oxidation state of III

(44) Cammack, R.; Bagyinka, C.; Kovacs, K. L. *Eur. J. Biochem.* **1989**, *182*, 357–62.
(45) Teixeira, M.; Moura, I.; Xavier, A. V.; Huynh, B. H.; DerVartanian, D. V.; Peck, H. J.; LeGall, J.; Moura, J. J. *J. Biol. Chem.* **1985**, *260*, 8942–50.
(46) Hyman, M. R.; Seefeldt, L. C.; Arp, D. J. *Biochim. Biophys. Acta* **1988**, *957*, 91–6.
(47) Kojima, N.; Fox, J. A.; Hausinger, R. P.; Daniels, L.; Orme-Johnson, W. H.; Walsh, C. *Proc. Natl. Acad. Sci. U.S.A.* **1983**, *80*, 378–82.
(48) Hatchikian, C. E.; Traore, A. S.; Fernandez, V. M.; Cammack, R. *Eur. J. Biochem.* **1990**, *187*, 635–43.
(49) Zöphel, A.; Kennedy, M. C.; Beinert, H.; Kroneck, P. M. H. *Eur. J. Biochem.* **1991**, *195*, 849–56.

**Table IV.** Analysis of Unfiltered EXAFS Data[a]

| redox state | no. of shells | $N$ | $r$ (Å) | $\Delta\sigma^2$ ($\times 10^3$ Å$^2$) | correl >0.6 | $R$ |
|---|---|---|---|---|---|---|
| form A(1) | 1 | 5 | Ni–N = 2.033(5) | 0.2 | | 1.552 |
| | 2 | 4 | Ni–N = 2.010(9) | 6.8 | | 1.319 |
| | | 1 | Ni–S = 2.209(6) | −1.6 | | |
| form A(2) | 1 | 4 | Ni–S = 2.206(4) | 7.3 | | 1.448 |
| | 2 | **3** | **Ni–N = 1.976(8)** | **0.6** | $r_S/\sigma_N$ = **−0.61** | 1.316 |
| | | **2** | **Ni–S = 2.226(7)** | **3.5** | | |
| | | 2 | Ni–N = 1.973(11) | −0.7 | $r_N/\sigma_S$ = 0.62 | 1.293 |
| | | 3 | Ni–S = 2.221(6) | 6.4 | | |
| form B(1) | 1 | 5 | Ni–N = 2.054(5) | −1.9 | | 3.419 |
| | 2 | 3 | Ni–N = 1.949(18) | 2.6 | | 3.016 |
| | | 2 | Ni–S = 2.234(4) | −3.5 | | |
| form B(2) | 1 | 4 | Ni–S = 2.219(4) | 6.3 | | 1.448 |
| | 2 | **3** | **Ni–N = 1.959(8)** | **3.4** | | **1.305** |
| | | **2** | **Ni–S = 2.239(4)** | **2.2** | | |
| SI | 1 | 4 | Ni–S = 2.240(5) | 6.6 | | 1.778 |
| | 2 | **2** | **Ni–N = 2.008(9)** | **−3.3** | | **1.712** |
| | | **2** | **Ni–S = 2.260(6)** | **0.3** | | |
| | | 2 | Ni–N = 2.033(24) | 3.6 | $r_N/r_S$ = −0.68 | 1.721 |
| | | 3 | Ni–S = 2.244(9) | 5.9 | | |
| form C(1) | 1 | 6 | Ni–N = 2.060(5) | −4.5 | | 4.182 |
| | 2 | 3 | Ni–N = 2.057(12) | −6.6 | $r_N/r_S$ = −0.71 | 3.991 |
| | | 2 | Ni–S = 2.212(21) | 1.6 | | |
| form C(2) | 1 | 4 | Ni–S = 2.233(3) | 6.0 | | 1.139 |
| | 2 | **2** | **Ni–N = 2.013(7)** | **−1.7** | | **1.146** |
| | | **2** | **Ni–S = 2.249(5)** | **0.4** | | |
| SR | 1 | 4 | Ni–S = 2.237(3) | 5.8 | | 1.250 |
| | 2 | **2** | **Ni–N = 2.030(11)** | **−1.1** | $r_N/\sigma_S$ = **0.62** | **1.217** |
| | | **2** | **Ni–S = 2.244(6)** | **1.8** | $r_S/\sigma_N$ = **−0.62** | |
| | | 2 | Ni–N = 2.077(20) | 2.6 | $r_N/r_S$ = −0.76 | 1.202 |
| | | 3 | Ni–S = 2.228(6) | 5.1 | $\sigma_S/\sigma_N$ = −0.86 | |

[a] Terms are defined in Table III.

**Table V.** Proposed Redox Schemes[a]

| obsd phenomenon | $E_m$ (mV vs NHE, pH 7.0) | proposal A | proposal B |
|---|---|---|---|
| EPR of Ni A | −150 | Ni(III) | Ni(III) |
| EPR of Ni B | | Ni(III) | Ni(III) |
| EPR silent intermediate | | Ni(II) | Ni(II) |
| appearance of Ni signal C | −270 | Ni(I) | Ni(III) |
| disappearance of Ni signal C | −390 | Ni(0) | Ni(II) |
| reductive activation | −310 | | |
| oxidative deactivation | −133 | | |

[a] Adapted from refs 21 and 26.

to the oxidized forms of the enzyme. Reduction of Ni(III) to Ni(II) accounts for the formation of the EPR silent intermediate. Further reduction of Ni(I) gives rise to the formation of another EPR active state (form C), and reduction to Ni(0) gives the reduced and EPR silent state. One problem associated with these scheme is the involvement of four oxidation states for a single Ni center within a span of 400 mV. This constitutes unprecedented redox chemistry for Ni.

One-electron redox chemistry is well-established for first-row transition metals, including Ni.[50-53] Proposal B has the advantage that it uses only two oxidation states of Ni. However, a problem arises in accounting for the EPR silent intermediate. All of the EPR active sites are assigned a formal oxidation state of Ni(III). Originally, it was posulated that this Ni(III) site could couple to an Fe,S cluster in the enzyme.[45] However, when Mössbauer experiments failed to reveal a paramagnetic Fe,S cluster at the

(50) Kruger, H. J.; Peng, G.; Holm, R. H. *Inorg. Chem.* **1991**, *30*, 734–42.
(51) Nag, K.; Chakravorty, A. *Coord. Chem. Rev.* **1980**, *33*, 87–147.
(52) Haines, R. I.; McAuley, A. *Coord. Chem. Rev.* **1981**, *39*, 77–119.
(53) Lappin, A. G.; McAuley, A. *Adv. Inorg. Chem.* **1988**, *32*, 241–95.

**Table VI.** XAS Edge Analysis in Metalloproteins

| protein | formal oxidation state change | edge shift (eV) | redox site | ref |
|---|---|---|---|---|
| galactose oxidase | Cu(III) → Cu(I) | ~0 | ligand | 55 |
| carbon monoxide dehydrogenase | Ni(III) → Ni(II) | ~0 | Fe, S cluster | 56 |
| sulfite oxidase | Mo(VI) → Mo(V) | 0.5 | ? | 57 |
| | Mo(V) → Mo(IV) | 0.5 | ? | |
| Mn OEC | | | | |
| $S_1 \rightarrow S_2$ | | 0.8 | metal | 58, 59 |
| $S_2 \rightarrow S_3$ | | ~0 | ligand | |
| cobalamin | Co(II) → Co(I) | 1.0 | metal | 60 |
| | Co(III) → Co(II) | 1.5 | | |
| cytochrome oxidase | $Cu_{a3}$(II) → $Cu_{a3}$(I) | 1.3 | metal | 61 |
| CO dehydrogenase | Ni(III) → Ni(II) | 1.42 | metal | 62 |
| cytochrome oxidase | Cu(II) → Cu(I) | 1.5 | ? | 63 |
| cytochrome oxidase | Fe(III) → Fe(II) | 2.2 | metal | 63 |
| stellacyanin | Cu(II) → Cu(I) | 2.0 | metal | 64 |
| plastocyanin | Cu(II) → Cu(I) | 2.2 | metal | 63 |
| xanthine oxidase | Mo(VI) → Mo(IV) | 3.1 | metal | 65 |

potential associated with the silent intermediate, the model was modified to involve reduction to Ni(II) followed by re-oxidation to Ni(III).[54] A final reduction to Ni(II) accounts for the EPR silent reduced form.

Either of these schemes imply structural changes in the Ni site that may be probed by X-ray absorption spectroscopy. A large decrease in oxidation state (proposal A) implies a large change in electron density at the metal, and it should be accompanied by a significant shift in the Ni K-edge energy and a lengthening of the Ni–ligand bonds. Proposal B would involve similar changes on a much smaller scale, but it must also involve a structural change in the Ni site that is sufficient to allow a site that is reduced at one potential to become reoxidized at a *lower* potential.

X-ray absorption edge energy, which is a sensitive measure of the charge residing on the metal center, is a good monitor of metal-centered redox processes. Edge energy shifts have been widely employed to monitor redox chemistry in metalloenzymes. The results from several metalloprotein studies are shown in Table VI. In general, shifts of ≤1 eV indicate that the redox chemistry involved is not localized on the metal center. Recently, this approach was used to examine the redox chemistry of the Cu site in galactose oxidase.[55] The lack of a significant Cu K-edge energy shift between the oxidized and reduced forms of the protein demonstrated that the redox chemistry was not metal-centered and implicated another redox active site. The crystal structure of the protein subsequently revealed a novel thioether composed of a cysteine and a tyrosinate ligand of the Cu site that is likely to be involved in the redox process.[66]

Particularly relevant to this study of the redox chemistry of the Ni center in $H_2$ase is a recent result from a study of the XAS

(54) Teixeira, M.; Moura, I.; Fauque, G.; DerVartanian, D. W.; LeGall, J.; Peck, H. D., Jr.; Moura, J. J. G.; Huynh, B. H. *Eur. J. Biochem.* **1990**, *189*, 381–6.
(55) Clark, K.; Penner-Hahn, J. E.; Whittaker, M. M.; Whittaker, J. W. *J. Am. Chem. Soc.* **1990**, *112*, 6433–6434.
(56) Tan, G. O.; Ensign, S. A.; Ciurli, S.; Scott, M. J.; Hedman, B.; Holm, R. H.; Ludden, P. W.; Korszun, Z. R.; Stephens, P. J.; Hodgson, K. O. *Proc. Natl. Acad. Sci. U.S.A.* **1992**, *89*, 4427–31.
(57) Cramer, S. P.; Gray, H. B.; Rajagopalan, K. V. *J. Am. Chem. Soc.* **1979**, *101*, 2772–4.
(58) McDermott, A. E.; Yachandra, V. K.; Guiles, R. D.; Cole, J. L.; Dexheimer, S. L.; Britt, R. D.; Sauer, K.; Klein, M. P. *Biochemistry* **1988**, *27*, 4021–31.
(59) Goodin, D. B.; Yachandra, V. K.; Britt, R. D.; Sauer, K.; Klein, M. P. *Biochim. Biophys. Acta* **1984**, *767*, 209–16.
(60) Wirt, M. D.; Sagi, I.; Chen, E.; Frisbie, S. M.; Lee, R.; Chance, M. R. *J. Am. Chem. Soc.* **1991**, *113*, 5299–304.
(61) Powers, L.; Blumberg, W. E.; Chance, B.; Barlow, C. H.; Leigh, J. S., Jr.; Smith, J.; Yonetani, T.; Vik, S.; Peisach, J. *Biochim. Biophys. Acta* **1979**, *546*, 520–38.
(62) Cramer, S. P.; Eidsness, M. K.; Pan, W.-H.; Morton, T. A.; Ragsdale, S. W.; DerVartanian, D. V.; Ljungdahl, L. G.; Scott, R. A. *Inorg. Chem.* **1987**, *26*, 2477–9.

of *Rhodospirillum rubrum* carbon monoxide dehydrogenase.[56] Like $H_2$ase, this enzyme contains both Ni and an Fe,S cluster and has redox chemistry that has been attributed to Ni primarily on the basis of changes in EPR spectra. These researchers report that during the reduction of the enzyme, little change is observed in the Ni K-edge, although changes are observed in the Fe K-edge, leading to the conclusion that "the additional electron does not reside in primarily Ni-derived orbitals and that there is no significant structural rearrangement upon oxidation/reduction."

A shift in the K-edge X-ray absorption edge energy of a metal arises from a change in the charge residing on the metal.[38,67,68] The charge on the metal center is determined by a combination of two factors: the oxidation state of the metal and the ability of the ligands to reduce the positive charge on the metal through covalent interactions. From model studies of Ni complexes where metal-centered redox chemistry is well-established, varying the oxidation state from III to II leads to shifts in the edge energy of 1–2 eV, while reduction from Ni(II) to Ni(I) leads to edge energy shifts of 2–3 eV.[38,39,69] Thus, in the absence of changes in the ligand environment of the Ni center in $H_2$ase, metal-centered redox chemistry involving reduction of Ni(III) to Ni(I) should give rise to edge energy shifts of 3–5 eV between forms B and C.

The most striking feature of the $H_2$ase Ni K-edge XAS spectra is the lack of sensitivity to the oxidation state of the enzyme as determined by the EPR spectrum of the Ni center. The edges shown in Figure 2 do not exhibit a significant shift to lower energy upon reduction of the enzyme. Within the precision of the results (±0.2 eV), the edge energies obtained from the form B, SI, form C, and R spectra are identical. Since the EXAFS analysis rules out a major change in the ligand environment of the protein, a metal-centered reduction involving a change in oxidation state of Ni from III to I is ruled out. The more modest oxidation state changes featured in proposal B are not supported by the edge data, but they could be accommodated by a highly covalent system, such as nickel dithiolenes.[38] However, no evidence is found to support a structural change that would be necessary to account for the reoxidation of the Ni site at a lower potential that is a feature of proposal B.

Although XAS cannot assign an oxidation state to the Ni center, it is clear that the oxidized enzyme (forms A and B) and the reduced and active enzyme (form C), as well as the EPR silent forms, contain Ni centers with comparable electron density. In the absence of change in the ligand environment, this indicates that all of the Ni centers exist in the same oxidation state. An attractive feature of proposal B is the fact that both forms B and C have the same oxidation state, Ni(III). However, the chemistry of the reduced form of the enzyme includes the binding of CO, a feature commonly associated with reduced Ni centers and one that has not been observed to occur in oxidized, formally Ni(III) complexes. Given the fact that Ni(II) complexes are known that bind CO,[70] the XAS data are consistent with a model that involves a Ni site that has at least the electron density typical of Ni(II) complexes. A recent investigation of the magnetic properties of the Ni site in the EPR silent intermediate of *Desulfovibrio baculatus* $H_2$ase concluded that it is diamagnetic—a result that demands that the site is low-spin Ni(II).[71] Since the edge energy is essentially constant from form B to the fully reduced enzyme, the XAS spectra (including the Ni–S bond distances, vide infra), the magnetic properties, and the chemistry of the Ni center are all consistent with a low-spin Ni(II) center in all forms of the enzyme.

Two samples of $H_2$ase poised in form A have an edge energy that is 0.6–1.1 eV higher in energy than is observed for B, which has the same formal oxidation state in both of the proposed redox schemes. The Ni center in form A may be slightly more electron deficient than the Ni centers in enzyme samples poised at other redox levels. One possibility is that an S-donor ligand has been lost or replaced by an O- or N-donor ligand. Although the fits of the EXAFS data for form A would appear to support this possibility (the N-only fit more closely approximates the data for this sample than any other), the lack of a change in the post-edge XANES data, as well as only small changes in the edge height (which increases for decreases in S-donor ligands[38] and is not at a maximal for form A), argues against this possibility.

Alternatively, the shift in edge energy to higher values may indicate a modification of one of the S-donor ligands in a manner that would render it a poorer electron donor, thus increasing the charge on Ni slightly. One possibility would be the oxidation of a thiolate ligand to a sulfenato or sulfinato ligand, as suggested by model chemistry.[72] Such a modification would be expected to give rise to an S-donor ligand that is a poorer electron donor than a thiolate but would not necessarily be detected by EXAFS since the Ni–S bonds in a model compound featuring one sulfinato and one thiolato ligand differ by only 0.027(2) Å.[72]

The analysis of the EXAFS data does not reveal any significant change in the ligand environment of the Ni in *T. roseopersicina* $H_2$ase as a function of redox state of the enzyme. The ligand environment of the Ni center in all five redox levels is the same as previously reported from a study of the XAS spectrum of form C[33] and is composed of a mixture of 3 ± 1 N(O)-donor ligands and 2 ± 1(Cl)-donor ligands. There is little change in the Ni–ligand bond lengths, which might be expected to accompany metal-centered redox processes. The Ni–S distances obtained from the fits are essentially identical at 2.23 ± 0.03 Å, and the Ni–N(O) distances exhibit only a small variation, 2.00 ± 0.06 Å. In contrast, the bond lengths reported for an isoleptic pair of Ni(III/II) model complexes with an $N_2S_4$ donor atom set, $Ni(pdtc)^{-/2-}$, exhibit an increase of 0.14 Å in the average Ni–S distance and an average increase of 0.01 Å in the average Ni–N distance upon reduction.[73]

Although a mixed-ligand Ni environment has not been found from the analysis of XAS spectra in other Fe,Ni $H_2$ases, the data obtained for *T. roseopersicina* $H_2$ase cannot be fit using a single shell of S scattering atoms. The Ni ligand environment found in *T. roseopersicina* $H_2$ase is consistent with that found in the Ni,Fe,Se $H_2$ase *D. baculatus*.[24] The mixed-ligand environment found in this study is also supportive of a proposed Ni site based on the amino acid sequence conservation observed in a number of $H_2$ases and site-directed mutagenesis studies of some of these residues.[3]

In all of the enzymes examined to date, S-donors at ca. 2.2 Å have been identified, although the number of S scattering atoms reported generally varies from ca. 2 to 4.[33,39,74–78] The Ni–S distance found for all of the redox levels of the enzyme (average

(63) Hu, V. W.; Chan, S. I.; Brown, G. S. *Proc. Natl. Acad. Sci. U.S.A.* **1977**, *74*, 3821–5.
(64) Peisach, J.; Powers, L.; Blumberg, W. E.; Chance, B. *Biophys. J.* **1982**, *38*, 277–85.
(65) Tullius, T. D.; Kurtz, D. M., Jr.; Conradson, S. D.; Hodgson, K. O. *J. Am. Chem. Soc.* **1979**, *101*, 2776–9.
(66) Ito, N.; Phillips, S. E. V.; Stevens, C.; Ogel, Z. B.; McPherson, M. J.; Keen, J. N.; Yadav, K. D. S.; Knowles, P. F. *Nature* **1991**, *350*, 87–90.
(67) Manthiram, A.; Sarode, P. R.; Madhusudan, W. H.; Gopalakarishnan, J.; Rao, C. N. R. *J. Phys. Chem.* **1980**, *84*, 2200–3.
(68) Sarode, P. R.; Ramasesha, S.; Madhusudan, W. H.; Rao, C. N. R. *J. Phys. C* **1979**, *12*, 2439–45.
(69) Furenlid, L. R.; Renner, M. W.; Szalda, D. J.; Fujita, E. *J. Am. Chem. Soc.* **1991**, *113*, 883–92.
(70) Saint-Joly, C.; Mari, A.; Gleizes, A.; Dartiguenave, M.; Dartiguenave, Y.; Galy, J. *Inorg. Chem.* **1980**, *19*, 2403–10.
(71) Wang, C. P.; Franco, R.; Moura, J. J. G.; Moura, I.; Day, E. P. *J. Biol. Chem.* **1992**, *267*, 7378–80.
(72) Kumar, M.; Colpas, G. J.; Day, R. O.; Maroney, M. J. *J. Am. Chem. Soc.* **1989**, *111*, 8323–5.
(73) Krüger, H.-J.; Holm, R. H. *J. Am. Chem. Soc.* **1990**, *112*, 2955–63.
(74) Maroney, M. J.; Colpas, G. J.; Bagyinka, C. *J. Am. Chem. Soc.* **1990**, *112*, 7067–8.
(75) Whitehead, J. P.; Colpas, G. J.; Bagyinka, C.; Maroney, M. J. *J. Am. Chem. Soc.* **1991**, *113*, 6288–9.
(76) Scott, R. A.; Wallin, S. A.; Czechowski, M.; DerVartanian, D. V.; LeGall, J.; Peck, H. D., Jr.; Moura, I. *J. Am. Chem. Soc.* **1984**, *106*, 6864–5.
(77) Scott, R. A.; Czechowski, M.; DerVartanian, D. V.; LeGall, J.; Peck, H. D., Jr.; Moura, I. *Rev. Port. Quim.* **1985**, *27*, 67–70.

Ni–S = 2.23 Å from Table III) is slightly longer than expected for low-spin (S = 0) planar four-coordinate thiolate complexes (2.16–2.21 Å)[79] and considerably shorter than observed in six-coordinate thiolate complexes (2.39–2.53 Å).[73,80–82] The average Ni–S bond length in the enzyme is more comparable to those found in five-coordinate trigonal-bipyramidal models (2.25–2.33 Å).[83,84] The combination of similar bond lengths and a similar ligand environment ($N_3S_2$) in one series of model complexes, Ni(terpy)$(SR)_2$, gives rise to XAS spectra that are strikingly similar to those observed in the $H_2$ase.[84]

The addition of a fourth N- or O-donor ligand to the Ni environment is Ni(terpy)$(SR)_2$ complexes to form six-coordinate complexes (Ni(terpy)L$(SR)_2$) has well-defined effects on the Ni–ligand distances, lengthening the average Ni–N bond length by ca. 0.01–0.06 Å and the average Ni–S bond length by ca. 0.1–0.2 Å.[83,84] These structural changes give rise to obvious effects in the EXAFS spectra of these models.[84] The EXAFS spectra of the six-coordinate models are distinct from the spectra obtained for the *T. roseopersicina* $H_2$ase Ni site. Thus, the EXAFS analysis of the structure of the Ni site is most consistent with a trigonal-bipyramidal Ni site composed of 3 N(O)-donor ligands and 2 S-donor ligands.

Nonetheless, the edges of the samples are most consistent with a six-coordinate Ni site. Two possible explanations involving an additional sixth ligand are plausible. First, a weakly bound sixth ligand could be present at a much longer distance. There is evidence for an S scatterer at a distance of 2.4–2.7 Å in many of the EXAFS spectra. However, unlike the Ni–N and Ni–S distances determined in the two shell fits, the additional Ni–S distance for the third shell sulfur atom shows some variability from sample to sample. Further, fits generated using unfiltered data are not significantly improved by the addition of a long Ni–S vector. Thus, not much confidence in the Ni–S distance for the long S scattering atom is warranted. However, the possibility that a long Ni–S interaction might account for the appearance of the Ni K-edge spectra remains. Second, for the SI, form C, and R samples, the possibility of a $H^-$ or $H_2$ Ni ligand exists. Such a proposal is consistent with ENDOR spectra obtained from EPR active forms of *Desulfovibrio gigas* $H_2$ase.[85] If such a ligand were present, it would not be detected in the EXAFS spectrum because of the small backscattering cross-section of H. It would, however, contribute to the symmetry of the complex, as reflected in the edge structure. In either case, the addition of another ligand must constitute a weak interaction because a strong interaction would be expected to give rise to a high-spin ($S = 1$) Ni center, which should feature bond lengths that are too long to be consistent with the EXAFS data.

## Conclusions

To the extent that the Ni site in the $H_2$ase from *Thiocapsa roseopersicina* is representative of those found in the class of Fe,Ni hydrogenases, several conclusions regarding the structure and function of the Ni center in Fe,Ni $H_2$ases may be drawn from this study:

1. There is no evidence from XAS to support a redox role for Ni in these enzymes. The absence of any significant change in edge energy coupled with the lack of a change in the ligand environment of the Ni center in all five oxidation states defined by the EPR spectrum of the Ni center is strong evidence that Ni-centered redox chemistry is not involved.

2. The XAS spectra are consistent with Ni sites in all of the samples studied that are either trigonal bipyramidal or six-coordinate with 2 ± 1 S(Cl)-donor ligands at 2.23 ± 0.03 Å and 3 ± 1 N(O)-donor ligands at 2.00 ± 0.06 Å.

3. The electron density changes associated with the redox process ascribed to Ni in several schemes, must be localized on other centers. The redox chemistry typical of Fe,S clusters is not sufficient to account for all of the redox processes observed. One possibility is that an as yet undetected redox active group, such as the one found in galactose oxidase,[66] might be involved. Another possibility that is consistent with the redox chemistry of nickel alkylthiolate complexes[72,79,86] is that the cysteine ligands are involved. Given the lack of change in the Ni–S bond lengths found in this study, it is unlikely that the redox changes are localized on one thiolate ligand, since this would be expected to give rise to changes in the Ni–S bond distance. A highly delocalized site involving all the thiolate ligands and the Ni center could account for redox changes involving one electron, such as suggested by proposal B in Table V. However, we find no evidence for a structural change in the Ni site that would account for the reoxidation of the center at a lower potential. It is conceivable that the change occurs at a ligand, rather than at the metal.

## Experimental Section

**Sample Preparations.** Cultures of *Thiocapsa roseopersicina BBS* were obtained from Dr. I. N. Gogotov, Institute of Soil Sciences, Puchino, Russia, and from Dr. Kornel Kovacs, Biological Research Institute, Hungarian Academy of Sciences, Szeged, Hungary. The bacteria were grown on a modified Pfenning's medium in 12.5-L-batch cultures, which were illuminated by incandescent lights. The cultures were harvested in the late logarithmic phase of growth by use of continuous flow centrifugation. The resulting cell paste was stored at −20 °C. In 300-g batches, the cell paste was converted to an acetone powder as previously described.[87] The $H_2$ase was purified from the acetone powder according to a minor modification of published procedures.[87] Final purification of the $H_2$ase was achieved by preparative gel electrophoresis.

Redox poised samples for the XAS studies were prepared by concentrating solutions containing 5 mg of $H_2$ase in 20mM Tris–HCl buffer (pH = 7.5) to 120 μL using a hollow fiber concentrator (Bio-Molecular Dynamics). These samples were then treated according to the procedures described below for each form of the $H_2$ase. The redox state of the Ni center in the enzyme during poising, as well as before and after exposure to synchrotron radiation, was monitored using EPR spectroscopy (Bruker ESP 300) at 77 K. The amount of protein in the samples was determined following the XAS experiments by diluting the whole sample to a known volume and measuring the absorbance at 220 and 280 nm. The extinction coefficients of the $H_2$ase at these two wavelengths were determined to be 895 000 and 106 000 $cm^{-1}$ $M^{-1}$, respectively, by analyzing samples of the enzyme for their amino acid content (vide infra). Metal analyses of several $H_2$ase samples, including those analyzed for amino acid content, were determined by graphite furnace atomic absorption spectroscopy.

**Form A:** Samples were poised in the oxidized and inactive form exhibiting Ni signal A ($g$ = 2.32, 2.23, 2.01) using a minor modification of a published procedure.[43] The procedure involved reducing the $H_2$ase under 10% $H_2/N_2$ until the samples exhibited only the EPR signal associated with the active form of the enzyme, form C. These reduced samples were then oxidized by the addition of a small amount of a concentrated solution of benzyl viologen (20 mM) and then by dilution to 4 mL with oxygenated buffer. The samples were reconcentrated and the dilution procedure was repeated as many times as necessary to maximize the form A EPR signal (at least ten times). The samples were concentrated to a final volume of ca. 35 μL by evaporation under a flow of $O_2$. The concentrations of the enzyme in the samples used for the XAS studies were 0.8 mM (A1) and 0.5 mM (A2 and A3). The samples were then loaded into polycarbonate holders for the XAS experiment and

(78) Lindahl, P. A.; Kojima, N.; Hausinger, R. P.; Fox, J. A.; Teo, B. K.; Walsh, C. T.; Orme-Johnson, W. H. *J. Am. Chem. Soc.* **1984**, *106*, 3062–55.
(79) Krüger, H. J.; Holm, R. H. *Inorg. Chem.* **1989**, *28*, 1148–55.
(80) Rosenfield, S. G.; Berends, H. P.; Gelmini, L.; Stephan, D. W.; Mascharak, P. K. *Inorg. Chem.* **1987**, *26*, 2792–7.
(81) Yamamoto, T.; Sekine, Y. *Inorg. Chim. Acta* **1984**, *83*, 47–53.
(82) Osakada, K.; Yamamoto, T.; Yamamoto, A.; Takenaka, A.; Sasada, Y. *Acta Crystallogr.* **1984**, *C40*, 85–7.
(83) Baidya, N.; Olmstead, M.; Mascharak, P. K. *Inorg. Chem.* **1991**, *30*, 929–37.
(84) Baidya, N.; Olmstead, M. M.; Whitehead, J. P.; Bagyinka, C.; Maroney, M. J.; Mascharak, P. K. *Inorg. Chem.* **1992**, *31*, 3612–19.
(85) Fan, C.; Teixeira, M.; Moura, J.; Moura, I.; Huynh, B. H.; Le, G. J.; Peck, H. D. J.; Hoffman, B. M. *J. Am. Chem. Soc.* **1991**, *113*, 20–4.
(86) Kumar, M.; Day, R. O.; Colpas, G. J.; Maroney, M. J. *J. Am. Chem. Soc.* **1989**, *111*, 5974–6.
(87) Kovacs, K. L.; Tigyi, G.; Alfonz, H. *Prep. Biochem.* **1985**, *15*, 321–34.

frozen. EPR spectra were then taken of the samples frozen in the XAS sample holders. Analysis of the EPR signals gave a sample composition of 78–95% form A with the remainder in form B, with the integration accounting for 85–91% of the Ni present in the samples. Long-term storage of the samples at 77 K affects the ratio of forms A and B in the samples. The effect of storage is to increase the amount of form A present and decrease the amount of form B in the sample. For example, a sample stored at 77 K for two months increased from ca. 80% to 95% form A. The composition of the samples reported was taken from EPR spectra obtained with a few days of collecting XAS data.

**Form B**: The $H_2$ase in the samples obtained from preparative gel electrophoresis was ca. 80% form B ($g$ = 2.33, 2.17, 2.01) and 20% form A. No method was found that would improve on this percentage of form B. Samples were concentrated as previously described, and the final concentration to ca. 35 μL was performed under a flow of Ar. The concentrations of the enzyme in the samples used for the XAS studies were 0.8 mM (B1) and 0.6 mM (B2). Samples were placed in XAS sample holders in air, and EPR spectra were taken and analyzed as described for form A. Samples for XAS data collection were prepared as close in time to data collection as possible because of the slow conversion of form B to form A upon long-term shortage.

**SI**: The EPR silent intermediate was prepared following the procedure described for the enzyme for *Chromatium vinosum*.[28] The sample was first reduced to form C under 10% $H_2/N_2$. The atmosphere was then changed to Ar, and the sample was incubated at 4 °C for 36 h. Final concentration to ca. 35 μL was achieved by evaporation under Ar flow. The concentration of the enzyme in the sample used for the XAS studies was 0.6 mM. The sample was quickly loaded into XAS sample holders in a chamber containing a 10% $H_2/N_2$ atmosphere (Coy Laboratories) and frozen. No EPR signal was detected from the sample used for XAS data collection.

**Form C**: The data reported for sample C(1) are from a previous study and are included in the text for comparison purposes. Sample C(2) was prepared by fully reducing the $H_2$ase to R (EPR silent) under 10% $H_2/N_2$ at room temperature. The sample was concentrated to ca. 35 μL under a flow of 10% $H_2/N_2$ and was reoxidized by the addition of 20 mM benzyl viologen in $H_2$-saturated buffer to a final concentration of 2 mM. The concentration of the enzyme in the sample used to collect XAS data was 0.9 mM. The sample was immediately loaded into an XAS sample holder under a 10% $H_2/N_2$ atmosphere and frozen. The only signal observed in the EPR spectrum of the sample was for form C ($g$ = 2.19, 2.14, 2.01), and integration of the signal using a 1.91 mM ($BzPh_3P$)-[Ni(pdtc)] solution in DMF as a standard accounted for 80% of the Ni in the sample.[33]

**R**: After concentration to a final volume of 35 μL (0.9 mM), the $H_2$ase was reduced through form C under 10% $H_2N_2$ until no EPR signal was detected. The sample was then loaded into XAS sample holders under a 10% $H_2/N_2$ atmosphere and frozen. Samples that were subsequently thawed under inert atmospheres retained activity in an $H_2$ evolution assay.[88] However, samples that were thawed in air underwent complete and irreversible inactivation. We conclude that fully reduced samples of the enzyme are extremely air sensitive. The sample in the XAS study was handled only under 10% $H_2/N_2$ atmosphere after reduction.

**Spectral Deconvolutions.** The composition of samples containing mixtures of forms A and B was determined by deconvolution of the EPR spectra. This was accomplished using standard techniques and the commercial software package SPSERV. Each form has a resolved $g_y$ EPR feature. Assuming 1.0 Ni/enzyme and that all of the Ni is EPR active in the oxidized samples, basis spectra were obtained from samples containing principally form A or form B eliminating the impurity signal using a fraction of the appropriate spectrum. The resultant spectrum containing a single EPR signal was renormalized by setting the double integral equal to 1.0.

EXAFS spectra for forms A and B corrected for the presence of a minor form were generated by using the results of the EPR deconvolutions.

**Amino Acid Analysis.** Three samples of $H_2$ase were analyzed following final purification by preparative gel electrophoresis. These samples were placed in 6 × 50 mm hydrolysis tubes that had been pyrolyzed for 4 h at 500 °C. The samples were dried in an evacuated centrifuge. The tubes were then placed in a hydrolysis vial to which 600 μL of 6 N HCl and 6 μL of liquefied phenol had been added. The hydrolysis vial and tubes were purged with Ar for 5 min. The vial was sealed and placed in an oven at 74 °C for 50 min. After completion of the hydrolysis, the vial was opened to release HCl vapor and the tubes were removed. Samples were reconstituted in 25 μL of 0.025% $K_3$EDTA, and 10-μL duplicates were loaded onto an Applied Biosystems 420A/130A derivatizer–analyzer. The amino acids were derivatized with phenylisothiocyanate (PITC) to form PTC-amino acid derivatives. The PTC-amino acids were resolved by using a reverse-phase microbore analytical column. Data were collected and analyzed with the Applied Biosystems 920A data module. Analyses for cysteine/cystine were carried out by oxidation to cysteic acid. This analysis was carried out as described above with the following modifications. The liquefied phenol was omitted from the hydrolyis vial and replaced with 2% (v/v) dimethyl sulfoxide. The derivatization cycle and 420A were modified as recommended by Applied Biosystems.

**XAS Data Collection.** Ni K-edge XAS data were collected on beamline X9A at the National Synchrotron Light Source at Brookhaven National Laboratory. The samples were contained in polycarbonate sample holders, which allowed XAS and EPR spectra to be measured without thawing the samples. For XAS measurements, the sample holders were inserted into slotted Al holders that were held near 80 K by contact with liquid $N_2$ in a cryostat. Data were collected under dedicated conditions between 8.1 and 9.2 keV by using a Si[111] crystal monochromator and a 1-mm vertical hutch aperture. Harmonic rejection was accomplished by use of a Ni focusing mirror left flat at an angle of 5 mrad. This arrangement has a theoretical bandpass of ca. 1.5–2.0 eV in the energy range employed. Edge energy determinations were reproducible to within ±0.2 eV. The energy scale of the spectra was calibrated to the first inflection point in the spectrum of Ni foil (8331.6 eV) using the procedure described below. Incident radiation ($I_0$) was measured using an $N_2$ filled ionization detector. Transmitted radiation ($I$) was measured using an Ar filled ionization detector. Fluorescence data were collected using a 13-element Ge detector (Canberra). No dead time corrections were required.

Scans were taken using a variable energy step size according to the resolution required in a particular region of the XAS spectra. The spectral regions (energy range) and energy step size used were as follows: pre-edge baseline region (8132–8312 eV), 5.0-eV steps; pre-edge XANES, edge, and post-edge XANES regions (8312–8382 eV), 0.5-eV steps; low-energy EXAFS region (8382–8582 eV), 2.0-eV steps; high-energy EXAFS region (8582–9232 eV), 5.0-eV steps.

The integrity of the samples after ~12 h exposure to synchrotron radiation was monitored in several ways. First, EPR spectra taken before and after exposure of the samples were compared. Second, the energy of the Ni K-edge was monitored on sequential scans to confirm the stability of the enzyme to reduction or oxidation in the X-ray beam. Third, samples poised in form C were analyzed by using a $H_2$ evolution assay.[88] None of the samples exhibited any significant change in any of the properties monitored.

**XAS Data Analysis.** The presence of a Ni mirror in the beam path on beamline X9A provides an internal calibration of the spectra. Data collected at a constant time/data point show an inverted absorption spectrum of the Ni mirror in the $I_0$ channel. The energy scale of the individual scans was calibrated to the minimum in $I_0$ (Ni absorption maximum) and then used to generate a spectrum consisting of the weighted sum of each of the 13 channels according to the procedure of Scott.[89] The individual scans were then summed, and the total fluorescence detector counts were divided by the total $I_0$ counts, yielding the summed XAS spectrum. The energy scale of the summed XAS spectrum was then externally calibrated to the Ni foil transmission spectrum.

To aid in the comparison of spectra taken on different samples, the signal to noise ratio of a given set of data was calculated. The edge jump height was taken as a measure of the signal. An estimate of the noise was taken by fitting a second-order curve to a section of the XAS data where all of the waves had damped out (approximately 8900 eV), and the value of the standard deviation ($\sigma$) was taken as a measure of the noise in a summed spectrum.

The XAS spectra were background corrected and normalized by using standard procedures.[90] For purposes of comparison, the edge energy is taken to be the energy at a normalized absorbance of 0.5. The edge energy obtained in this way from the raw data does not differ significantly from values obtained by a least-squares fitting of an arctangent or a Fermi function ($1/(1 + e^{-E})$) to the edge jump. An analysis of first derivative spectra led to values of the edge energy (peak maxima) that are ca. 1.0 eV higher in absolute value but show the same energy differences as the values determined by using the methods described above.

(88) Bagyinka, C.; Zorin, N. A.; Kovacs, K. L. *Anal. Biochem.* **1984**, *142*, 7–15.

(89) Scott, R. A. *Meth. Enzymol.* **1985**, *117*, 414–59.

(90) Scarrow, R. C.; Maroney, M. J.; Palmer, S. M.; Que, L., Jr.; Roe, A. L.; Salowe, S. P.; Stubbe, J. *J. Am. Chem. Soc.* **1987**, *109*, 7857–64.

The areas under the peaks assigned to 1s → 3d transitions were determined by subtracting a fit to the edge (arctangent or Fermi function) and integrating the difference spectrum. EXAFS data were corrected for detector efficiencies, absorbance by air and cryostat windows, and the variation with energy of the sample X-ray penetration depth.[90] Least-squares fits of the data over a $k$ range of 2–12.5 Å$^{-1}$ were performed as previously described.[33] Best fits were judged by minimizing $|\Delta\sigma^2| = |(\sigma^2_{fit} - \sigma^2_{model})|$ and $R$ ($R = [\Sigma k^6(\chi_c - \chi)^2/n]^{1/2}$, where the summation is performed over the $n$ data points in the range of $k$ = 2–12.5 Å$^{-1}$) using single-scattering EXAFS theory (eqs 1 and 2).[89]

$$\chi_c = \sum_{shells}\{NA[f(k)]k^{-1}r^{-2}e^{-2\sigma k^2}\sin(2kr + \alpha(k))\} \quad (1)$$

$$k = [4\pi m_e(E - (8340\text{ eV} + \Delta E))/h]^{1/2} \quad (2)$$

Empirical parameters used in generating the fits (amplitude reduction factors, Debye–Waller factors, $E_0$) were obtained from transmission data previously collected from model compounds, $[Ni(Im)_6](BF_4) = (Et_4N)_2[Ni(p\text{-}SC_6H_4Cl)_4]$.[33]

**Acknowledgment.** Funding for this work was provided by a grant from the NIH (GM-38829, M.J.M.). We thank the National Biostructures PRT, which is supported by a grant from the NIH (RR-01633), for beam-time allocations and access to equipment. We are also indebted to Prof. Robert Scarrow for providing a copy of his EXAFS analysis package, SEXAFS, to Cheryl Coté and the UMass MCB core facility for amino acid analysis, to Dr. Simon Albracht for providing information to us prior to publication, and to Dr. Syed Khalid for experimental support.

**Supplementary Material Available:** Fits to Fourier-filtered first coordination sphere EXAFS data, fits to unfiltered EXAFS data, and analysis of EXAFS data for spectra corrected for composition of forms A and B (45 pages). Ordering information is given on any current masthead page.